International Journal of Chemical Engineering Research.
ISSN 0975-6442 Volume 9, Number 2 (2017), pp. 153-161

http://www.ripublication.com

Infrared Spectral and Elastic Moduli study of Pr^{+3} doped Ni-Co-Zn ferrites via Normal Micelles Method

Ketan A Ganure, Vinod T Katkar, Laxman A Dhale, Kishan S Lohar*

Department of Chemistry, Srikrishna Mahavidyalaya Gunjoti, Omerga, Osmanabad Maharashtra, India 413 613.

**Corresponding Author*

Abstract

Normal micelle method is a well-defined reacting mixture for the synthesis of nano structured and functional ferrite particles of controlled size and shape having the general chemical formula $Ni_{0.6}Co_{0.2}Zn_{0.2}Fe_{2-x}Pr_xO_4$(x=0.00 to0.10 in the step of 0.025). The Fourier Transform Infrared Spectra (FT–IR) of the Ni–Co–Zn ferrite system have been analyzed in the frequency range of 4000–400cm[1]. The high frequency absorption band 'υ_1' around 620 cm^{-1} assigned to tetrahedral complex and low frequency absorption band 'υ_2' around 420 cm^{-1} assigned to octahedral complex. The force constant, bond length and Debye temperature were determined by infrared spectra analysis. The force constant, lattice constant and pore fraction have been used to investigate the elastic moduli such as Young's Modulus, Bulk Modulus, Rigidity Modulus.

Keywords: Normal micro-emulsion, Ni-Co-Zn Ferrites, Infra-Red, Elasticity.

1. INTRODUCTION

The nanocrystalline spinel ferrites have been studied extensively due to their potential applications in non-resonant devices, radio frequency circuits, high-quality filters, rod antennas, transformer cores, read-write heads for high speed digital tapes, and operating devices, magnetic drug delivery, magnetic fluid, high density information storage etc. [1-3]. Rare-earth elements have a vital role in the development of technology because they exhibit some important physical properties like luminescence [4-5], superconductivity [6], laser [7], etc. Mixed ferrites like Ni–Zn-ferrites and Co–Zn-ferrites appear to be the most important magnetic materials in this

family. Prior research also indicated improvement of soft magnetic property by doping in Ni–Zn-ferrite [8], which inspired the choice of the present ferrite. Ni–Co–Zn ferrites have been synthesized by an oxalate precursor method [9]. Some of these methods are Ceramic Method, Co-precipitation Method, Citrate Precursor Method, Sol–gel auto-combustion Method and Micro-emulsion method [10].

However, to the best of author's knowledge there is no work carried out in the literature regarding to the substitution Pr^{+3} doped Ni–Co–Zn-ferrite nanoparticles. Prepared by the normal micelle method. In the present work we decided to study the effect of Pr^{+3} on the structural and Elastic properties of Ni–Co–Zn with a chemical formula (x=0.00 to0.10 in the step of 0.025).

2. EXPERIMENTAL

Materials

The analytical grade reagent of Nickel nitrate ($Ni(NO_3)_2.6H2O$), Cobalt nitrate ($Co(NO_3)_2.6H_2O$), zinc nitrate ($Zn(NO_3)_2.6H_2O$), Ferric nitrate ($Fe(NO_3)_3.9H_2O$), Praseodymium nitrate ($Pr(NO_3)_3.5H_2O$), (Aldrich 97%) of Sodium doceyl sulphate (SDS) and Methyl amine and used in the synthetic reaction without any further treatment.

Synthesis of Pr^{+3}doped ferrite nanoparticles by normal micelles method

The normal micro-emulsion method, used to prepare the samples having the chemical composition $Ni_{0.6}Co_{0.2}Zn_{0.2}Fe_{2-x}Pr_xO_4$ (x=0.00 to0.10 in the step of 0.025). The AR grade corresponding metal nitrates were used as starting material and were mixed in a stoichiometric proportion in double distilled water. An aqueous solution of Sodium Doceyl Sulphate (SDS) added into the nitrate mixture with continuous stirring at temperature 45 °C, Methyl amine (40% in water) added; with maintain pH ≅ 9 at constant temperature. Dark brown precipitate formed and stirring continued for next 3 hours at temperature 60 °C, until the precipitate digested. The precipitate filtered through Wattman filter paper No. 41, the precipitate were washed with double distilled water and dried at room temperature, resulting a brown coloured powder.

3. RESULTS AND DISCUSSION

Infrared spectra Studies

Figure 1 shows FT–IR spectrum of investigated system in the range of 4000-400 cm^{-1}. The absorption bands obtained are in the expected range, which confirms the absorption band 'ν_1' around 600–620 cm^{-1} is assigned to the intrinsic stretching

vibrations of tetrahedral complexes and band 'ν_2' around 400–420 cm^{-1} is assigned as octahedral complexes which are characteristics features of spinel ferrites [11].

The higher frequency band 'υ_1' is nearly constant for the different Pr^{+3} ions substitutions. The lower frequency band 'υ_2' slightly shifts to higher frequency, increasing in the Pr^{+3} ions content, with obvious broadening.

This shifts can attributed to the decrease in metal–oxygen bond length due to the displacement of larger Pr^{+3} ions in the B–sites by smaller Fe^{+3} ions. The observed decrease in the band intensity with increasing in Pr^{+3}content can be due to perturbation occurring in Fe–O bands by substitutions of Pr^{+3} ions [12].

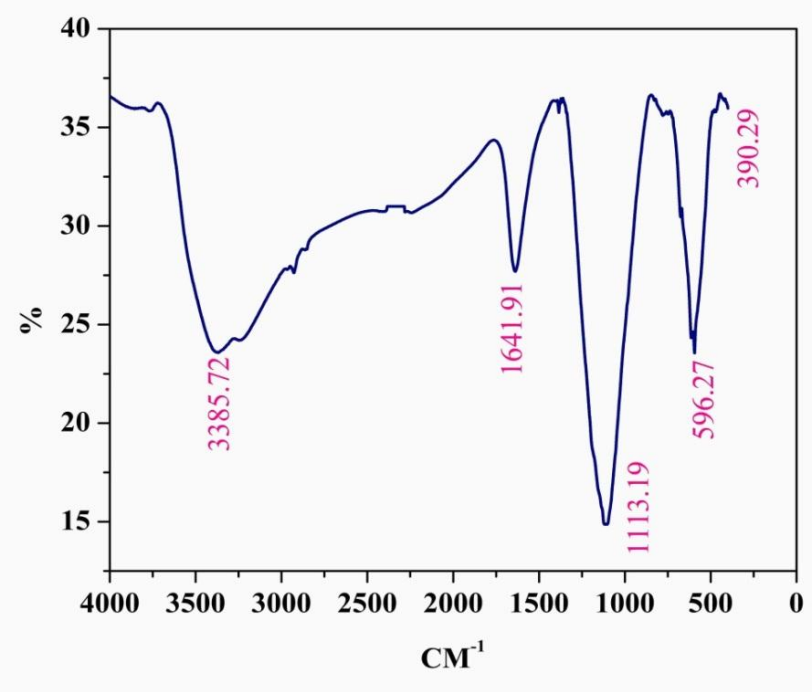

Figure 1: Infra-red Spectrum of $Ni_{0.6}Co_{0.2}Zn_{0.2}Fe_{2-x}Pr_xO_4$ (x=0.050)

The absorption peaks at 1642 cm^{-1} attributed to the absorbed water molecules and adsorbed or atmospheric CO_2 [13]. The adsorbed water molecule is assigned by bands around 3400 and 1600 cm^{-1}, which are assigned to the O–H stretching and H–O–H bending modes of vibration, respectively [14]. The absorption peaks 1094 cm^{-1} assigned to be deformation of C–H group [15].

The force constant for the tetrahedral site (K_T) and octahedral site (K_0) was estimated by employing the method suggested by 'Waldron' [20]

$$K_0 = \frac{0.942128 M_1 \nu_2^2}{(M_1 + 32)} \quad \textbf{(1)}$$

$$K_T = 0.04416\nu_1^2 M_2\left(\frac{V}{V+3}\right) \quad \textbf{(2)}$$

The force constant (K) is the mean of (K_T) and (K_0), it's second derivative of the potential energy with respect to inter-nuclear separation, the other independent parameters being kept constant. It receives its major contribution from short-order closed-shell repulsive forces rather than from coulomb-attractive forces at the ionic equilibrium positions. The force constant will therefore be more sensitive to a decrease in bond length than to an increase. [16].

Elastic property studies

Elastic moduli and Debye temperature were calculated through IR data and structural data of the presently investigated spinel ferrite samples [17, 18]. These elastic moduli were calculated using the values of lattice constant 'a', X-ray density 'dx', pore fraction 'f' and force constant 'K'. The value of Lattice constant 'a', X ray density 'dx', Bond lengths (R_A & R_B), Force constant 'K' are listed in Table 1.

Table 1 Lattice constant 'a', X ray density 'dx', Bond lengths (R_A & R_B), Force constant 'K' and Poisson's ratio 'σ' of $Ni_{0.6}Co_{0.2}Zn_{0.2}Fe_{2-x}Pr_xO_4$

(x=0.00, 0.025, 0.050, 0.075, 0.10)

Comp.	a_{obs} (Å)	dx (g/cm^3)	R_A	R_B	K_t(dyne/cm)	K_0(dyne/cm)	Poisson's ratio 'σ'
0.00	8.1134	5.863	0.3796	0.3039	179222	103838.2	1.2888
0.025	8.2808	5.565	0.3799	0.3041	175243	101348.5	1.2869
0.050	8.3621	5.430	0.3802	0.3042	177588	102238.3	1.2849
0.075	8.4128	5.402	0.3805	0.3043	180986	104186.9	1.2818
0.10	8.4646	5.350	0.3808	0.3045	183759	106106.7	1.2786

The elastic constants are of much importance because they elucidate the nature of binding forces and to understand the thermal properties of solids. The elastic moduli often used are Young's modulus, Bulk modulus, Rigidity modulus and Poisson's ratio. Among all the elastic constants of ferrites, Young's modulus is special interest because it is the decisive factor for the most widely employed core shapes, namely rods and rings [16]. The stiffness constant (C_{11}) calculated using relation [19],

The value, of stiffness constant (C_{11}) and (C_{12}) are calculated and described in Figure 2. The stiffness constants decrease with increase in Pr^{+3} ions content. The values of Poisson's ratio calculated using the relation discussed elsewhere [20] and the values are in Table 1. The values of Poisson's ratio are decreased with the increasing Pr^{3+} ions content. The other elastic moduli for cubic structure are calculated using following relation [21],

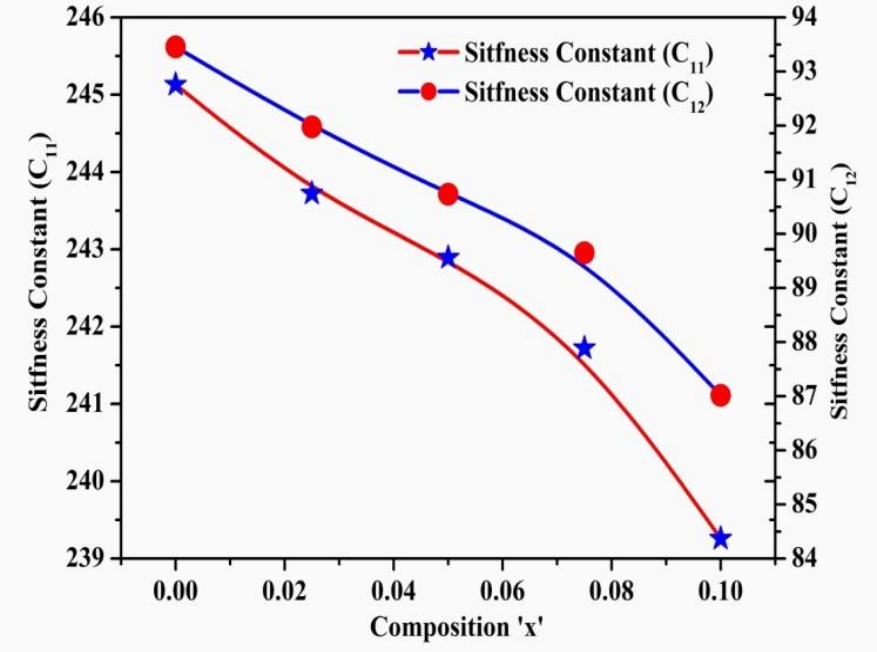

Figure 2: Variation of stiffness constant with Pr^{+3} Content.

The Young's modulus (E), Bulk Modulus (K) and Rigidity modulus (G_O) calculated by using above equations and variation is illustrated in Figure 3.

$$\text{Young's modulus (E)} = \frac{(C_{11}-C_{12})(C_{11}+2C_{12})}{(C_{11}+C_{12})} \quad \textbf{(3)}$$

$$\text{Bulk Modulus (K)} = \frac{1}{3}\left(C_{11}+C_{12}\right) \quad \textbf{(4)}$$

$$\text{Rigidity modulus } (G_O) = \frac{E}{2(\sigma+1)} \quad \textbf{(5)}$$

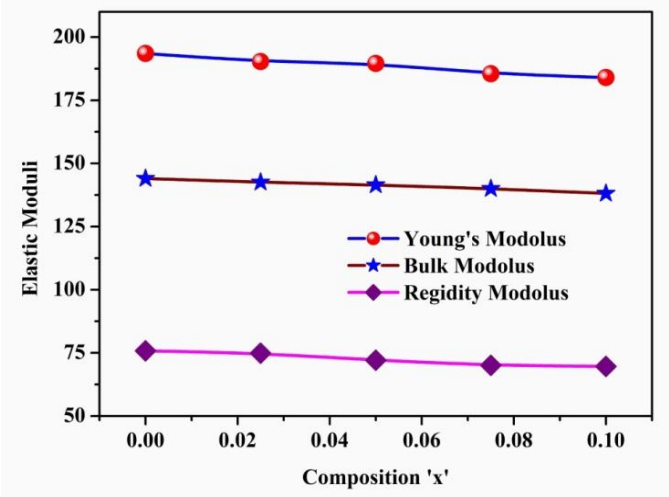

Figure 3: Variations of Elastic Moduli with Pr^{+3} Content.

Debye temperature *'θ_E'* calculated using formula;

$$\text{Debye temperature } (\theta_{E)} = \frac{h}{k}\left[\frac{3\rho q N_A}{4\Pi M}\right]^{1/3} \times V_m \qquad \textbf{(6)}$$

Where,

'h' is planks constant, k is Boltzmann's constant, M is molecular weight, 'q' is number if atom in the unit formula and V_m mean wave velocity.

The variation of Debye temperature (θ_E and θ_I) is decreases with Pr^{3+} ions substitution as shown in Figure 4. Debye temperature represent the temperature at which nearly all modes of vibration in solid are excited and decrease in Debye temperature implies the decrease in the rigidity of the ferrite.

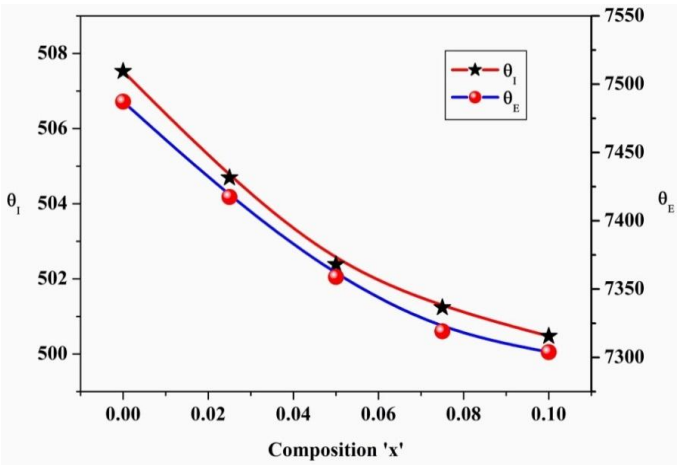

Figure 4: Variation of Debye Temperature (θ_I and θ_E) with Pr^{+3} Content.

4. CONCLUSION

Normal micelles method to prepare the Pr^{+3}-doped nanoferro spinle compounds having the general formula $Ni_{0.6}Co_{0.2}Zn_{0.2}Fe_{2-x}Pr_xO_4$ (x=0.00 to 0.10 in the step of 0.025). FT-IR shows two absorption bands 'ν_1' around 600-620 cm^{-1} is assigned to the intrinsic stretching vibrations of tetrahedral complexes and band 'ν_2' around 400-420 cm^{-1} is assigned as octahedral complexes. The bond lengths (R_A and R_B) increases with increase in Pr^{+3} content. The Poisson's ratio decreases with increase in Pr^{+3}content. Stiffness constants (C_{11} and C_{12}) decreases with increase in Pr^{+3}content. Variation of Elastic Moduli Young's modulus (E), Bulk modulus (K) and Rigidity modulus (G) increases as Pr^{+3}content increases. The variation of Debye temperatures (θ_E and θ_I) is decreases with Pr^{3+} content and decrease in the rigidity of the ferrite.

ACKNOWLEDGEMENT

The one of authors **Ketan A Ganure** and **Dr. Kishan. S. Lohar** is thankful to New Delhi, for providing financial support according to grant F.No.42-313 /2013.

REFERENCES

[1] Goldman, A.1984, "Understanding ferrites," American Ceramic Society Bulletin., 63(4), pp.582-585.

[2] Ravindranathan, P., & Patil, K. C. 1987, "Novel solid solution precursor method for the preparation of ultrafine Ni-Zn ferrites,' Journal of Materials Science, 22(9), pp.3261-3264.

[3] Igarash, H., & Okazaki, K. 1977, "Effects of Porosity and Grain Size on the Magnetic Properties of NiZn Ferrite," J. Am. Ceram. Soc, 60, pp.54-51.

[4] Yang, H., Seo, S., Abboudi, M., & Holloway, P. H., 2007, "Synthesis and luminescent properties of rare earth-doped Y^{+4} nanocrystalline powders." Journal of Ceramic Processing Research, 8(4), pp.256.

[5] Garskaite, E., Lindgren, M., Einarsrud, M. A., & Grande, T., 2010, "Luminescent properties of rare earth (Er, Yb) doped yttrium aluminium garnet thin films and bulk samples synthesised by an aqueous sol–gel technique," Journal of the European Ceramic Society, 30(7), pp.1707-1715.

[6] Meier, K., Cardoso-Gil, R., Schnelle, W., Rosner, H., Burkhardt, U., & Schwarz, U., 2010, "Thermal, Magnetic, Electronic, and Superconducting Properties of Rare-Earth Metal Pentagermanides $REGe_5$ (RE= La, Nd, Sm, Gd) and Synthesis of TbGe," Zeitschrift fur anorganische und allgemeine Chemie, 636(8), pp.1466-1473.

[7] R. Peters, K. Petermann, G. Huber, 2010, "Growth Technology and Laser Properties of Yb-Doped Sesquioxides, in: P. Capper, P. Rudolph (Eds.), Crystal Growth Technology: Semiconductors and Dielectrics, Wiley-VCH Verlag GmbH & Co.KGaA, Weinheim, pp. 267–282.

[8] Modak S, Ammar M, Mazaleyrat F, Das S, Chakrabarti PK., 2009, "Enhanced Magnetic Behavior of Chemically Prepared Multiferroic Nanoparticles of $GaFeO_3$ in $(GaFeO_3)$ 0.50 $(Ni_{0.4}Zn_{0.4}Cu_{0.2}Fe_2O_4)$ 0.5 Nanocomposite." J Alloys Compd, 473, pp.15–9.

[9] Want, B. 2011, "Single crystal growth and characterization of lanthanum–neodymium oxalate octahydrate," Journal of Crystal Growth, 335(1), pp. 90-93.

[10] Shirsath, S. E., Jadhav, S. S., Toksha, B. G., Patange, S. M., & Jadhav, K. M., 2011, "Influence of Ce^{4+} ions on the structural and magnetic properties of $NiFe_2O_4$," Journal of Applied Physics, 110(1), pp.013914.

[11] Waldron, R. D, 1955, Infrared spectra of ferrites. Physical review, 99(6), 1727.

[12] Gabal, M. A., & Al Angari, Y. M, 2009, "Effect of chromium ion substitution on the electromagnetic properties of nickel ferrite," Materials Chemistry and Physics, 118(1), pp.153-160.

[13] X. Ma. H. Sum, H. He. M. Zheng, 2007, "Competitive reaction during decomposition of hexachlorobenxene over ultra-fine C-Fe composite oxide catalyst," Catalysis Lattters 119 (1-2) pp.142-147.

[14] M. Mozaffari, S. Manouchehri, M.H. Yousefi, J. Amighian, 2010, "The effect of solution temperature on crystallite size and magnetic properties of Zn substituted Co ferrite nanoparticles", Journal of Magnetism and Magnetic Materials 322. pp.383–388.

[15] Z. Yue, L. Li, J. Zhou, H. Zhang, Z. Gui, 1199, "Preparation and Characterization of NiCuZn ferrite nanocrystaline powders by auto combustion of nitrate-citrate gels, Material Science and Engineering; B 64 (1) pp.68-72.

[16] K. B. Modi, S. J. Shah, N. B. Pujara, T. K. Pathak, N. H. Vasoya, I. G. Jhala. 2013, "Infrared spectral evolution, elastic, optical and thermodynamic properties study on mechanically milled $Ni_{0.5}Zn_{0.5}Fe_2O_4$ spinel ferrite," Journal of Molecular Structure 1049, pp.250–262.

[17] Birajdar, A. A., Shirsath, S. E., Kadam, R. H., Mane, M. L., Mane, D. R., & Shitre, A. R. 2012, "Permeability and magnetic properties of Al^{3+} substituted $Ni_{0.7}Zn_{0.3}Fe_2O_4$ nanoparticles. *Journal of Applied Physics*, *112*(5), pp.053908.

[18] Pathak, T. K., Buch, J. J. U., Trivedi, U. N., Joshi, H. H., & Modi, K. B. 200, "Infrared spectroscopy and elastic properties of nanocrystalline Mg–Mn ferrites prepared by co-precipitation technique," Journal of nanoscience and nanotechnology, 8(8), pp.4181-4187.

[19] Modi K. B., Gajera J. D., Pandya M. P., Vora H. G., Joshi H. H. 2004, "Far-infrared spectral studies of magnesium and aluminum co substituted lithium ferrites," Pramana, journal of physics. 62, pp.1173-1180.

[20] Bhatu S. S., Lakhani V. K., Tanna A. R., Varsoya N. H., Buch J. U., Sharma P. U., Trivedi U. N., Joshi H. H., Modi K. B., 2007, "Effect of nickel substitution on structural, infrared and elastic properties of lithium ferrite," Ind. J. Pure Appl. Phys. pp.45:596.

[21] Patil V. G., Shrisath Sagar E., More S. D., Shukla S. J., Jadhav K. M., 2009, "Effect of zinc substitution on structural and elastic properties of cobalt ferrite," J. Alloys Compd. 488, pp.199-203.